ELSEVIER
Chemical Engineering Journal 120 (2006) 181–191
Chemical Engineering Journal
www.elsevier.com/locate/cej

Residence time distribution of a purely viscous non-Newtonian fluid in helically coiled or spatially chaotic flows

C. Castelain [a], P. Legentilhomme [b,*]

[a] *Laboratoire de Thermocinétique UMR CNRS 6607, Ecole Polytechnique de l'Université de Nantes, La Chantrerie, BP 50609, F-44306 NANTES Cedex 03, France*
[b] *Laboratoire GEPEA UMR CNRS 6144, Institut Universitaire de Technologie, Département Génie Chimique, BP 420, F-44606 Saint-Nazaire Cedex, France*

Received 2 September 2005; received in revised form 13 April 2006; accepted 19 April 2006

Abstract

This work is dedicated to an experimental study of residence time distributions (RTD) of a pseudoplastic fluid in different configurations of helically coiled or chaotic systems. The experimental system is made up of a succession of bends in which centrifugal force generates a pair of streamwise Dean cells. Fluid particle trajectories become chaotic through a geometrical perturbation obtained by rotating the curvature plane of each bend of $\pm 90^{\circ}$ with respect to the neighboring ones (alternated or twisted curved ducts). Different numbers of bends, ranging from 3 to 33, were tested. RTD is experimentally obtained by using a two-measurement-point conductimetric method, the concentration of the injected tracer being determined both at the inlet and at the outlet of the device. The experimental RTD is modeled by a plug flow with axial dispersion volume exchanging mass with a stagnant zone. RTD experiments were conducted for generalized Reynolds numbers varying from 30 to 270. The Péclet number based on the diameter of the pipe is found to increase with the Reynolds number whatever the number of bends in the system. This reduction in axial dispersion is due to both the secondary Dean flow and the chaotic trajectories. Globally, the flowing fraction, which is one of the characteristic parameters of the model, increases with the Reynolds number, whatever the number of bends, to reach a maximum value ranging from 90% to 100%. For Reynolds numbers less than 200, the flowing fraction increases with the number of bends. The stagnant zone models fluid particles located close to the tube wall. The pathlines become progressively chaotic in small zones in the cross section and then spread across the flow as the number of bends is increased, allowing more trapped particles to move towards the tube center. Results have been compared with those previously obtained using Newtonian fluids. The values of the Péclet number are greater for the pseudoplastic fluid, the local change of apparent viscosity affecting the secondary flow. For pseudoplastic fluids, the apparent viscosity is lower near the wall and higher at the center of the cross section. The maximum axial velocity is flattened as the flow behavior index is reduced, inducing a decrease of the secondary flow in the central part of the pipe and an acceleration of it near the wall, which reduces the axial dispersion. These results are encouraging for the use of this system as continuous mixer for complex fluids in laminar regime, particularly for small Reynolds numbers.
© 2006 Elsevier B.V. All rights reserved.

Keywords: Residence time distribution; Dispersion; Pseudoplastic fluid; Helical coil; Chaotic flow

1. Introduction and literature survey

In continuous processes, many investigations are dedicated to the dispersion phenomenon in various systems in order to homogenize the residence time distribution, to increase mixing in order to minimize the temperature gradients in heating systems or to enhance the conversion rate in chemical reactors. Flow in straight tubes has been studied for a long time, notably by Taylor [1]. Techniques commonly used to enhance mixing often involve the generation of turbulent flows. In some cases, fluids with long molecular chains can be damaged by high shear stresses and turbulent mixing is also energy consuming. Furthermore, in many processes, it is very difficult to reach a turbulent flow regime due to the high apparent viscosity of certain viscous and/or non-Newtonian fluids.

In the laminar regime, for example in a straight tube, mixing is mainly driven by molecular diffusion. However, different mechanisms can induce a decrease of the axial dispersion. Some devices allow to improve mixing efficiency, such as static mix-

* Corresponding author. Tel.: +33 2 40 17 81 92; fax: +33 2 40 17 81 84.
E-mail address: patrick.legentilhomme@univ-nantes.fr (P. Legentilhomme).

1385-8947/$ – see front matter © 2006 Elsevier B.V. All rights reserved.
doi:10.1016/j.cej.2006.04.009

Nomenclature

C concentration of an injected tracer (mol m^{-3})
C_f friction factor
$C_1(t)$ concentration of an injected tracer at the inlet (mol m^{-3})
$C_2(t)$ concentration of an injected tracer at the outlet (mol m^{-3})
$C_{2calc}(t)$ calculated concentration of an injected tracer at the outlet (mol m^{-3})
$C'_1(t)$ normalized concentration of an injected tracer at the inlet
$C'_2(t)$ normalized concentration of an injected tracer at the outlet
C^* concentration of an injected tracer in the stagnant zone (mol m^{-3})
D tube diameter (m)
Dn Dean number, $\mathrm{Dn} = Re\sqrt{D/R_c}$
D_{ax} axial dispersion coefficient (m^2 s^{-1})
D_c coil diameter (m)
$\mathrm{Dn_g}$ generalized Dean number, $\mathrm{Dn_g} = Re_g\sqrt{D/R_c}$
f fraction of volume subjected to flow
$F(s)$ transfer function
G dimensionless group, $G = (KL)/\bar{W}$
k consistency index (Pa s^n)
K mass transfer coefficient between the flowing volume and the stagnant region (s^{-1})
L total length of the system (m)
n flow behavior index
P pressure (Pa)
Pe_D Péclet number based on the diameter of the system, $Pe_D = (\bar{W}D)/D_{ax}$
Pe_L Péclet number based on the total length of the system, $Pe_L = (\bar{W}L)/D_{ax}$
Re Reynolds number, $Re = (\bar{W}D)/\nu$
RMS root mean square error between the experimental and the calculated response curves (%)
R_c mean curvature radius (m)
Re_g generalized Reynolds number, $Re_g = 8^{1-n}[4n/(3n+1)]^n[(\rho\bar{W}^{2-n}D^n)/k]$
t time (s)
$\bar{t}_s$ mean residence time (s)
$\bar{W}$ average axial velocity (m s^{-1})

Greek symbols
β dimensionless number, $\beta = Pe_L^2 + 4s\gamma Pe_L\bar{t}_s$
γ dimensionless number, $\gamma = f + [(G(1-f))/(\bar{t}_s s(1-f)+G)]$
μ dynamic viscosity (Pa s)
ν kinematic viscosity (m^2 s^{-1})
ξ dimensionless geometrical parameter
ρ fluid density (kg m^{-3})
τ_w wall shear stress (Pa)
ω pulsation of the Fourier series (rad s^{-1})

ers or helical ones for instance. For very viscous fluids, static mixers can induce prohibitive pressure drops.

In helical systems, mixing of Newtonian fluids has been the subject of many investigations. Dispersion processes are often investigated, both theoretically and experimentally, using the concept of residence time distribution (RTD). For helical systems, in laminar flow, the presence of two contra-rotative vortices called Dean cells [2,3] due to the centrifugal force, increases transverse mixing and makes concentration distribution in the cross-sectional plane more uniform. Consequently, the axial dispersion is reduced. Erdogan and Chatwin [4] carried out a theoretical analysis of the effective dispersion in a curved duct using the velocity field determined by Dean [2,3]. They expressed the effective dispersion coefficient, D_{eff}, as the sum of a curvature-independent term, representing the solution obtained by Taylor [1] in a straight tube, and an additional one taking into account the curvature effects. From the works of Erdogan and Chatwin [4], it can be seen that D_{eff} is reduced by curvature effects only if the Schmidt number, Sc, is greater than 0.57, which is the case for all common liquids and most gases. Erdogan and Chatwin [4] conclude that the secondary flow induces a transverse mixing helping molecular diffusion in the mixing process. In this system, the mass transport perpendicular to the main flow is driven by both molecular diffusion and advection. The modification of the axial velocity profile due to the secondary flow induces a narrower residence time distribution compared with that obtained in a straight tube. Ruthven [5] derived a theoretical residence time distribution for ideal laminar flow through a helical tube when molecular diffusion can be neglected. He showed that, when the flow pattern is fully developed and for $Re \leq L/D \leq 1.5Re$ and $\mathrm{Dn} \leq 17$, the RTD becomes almost independent of curvature and Reynolds number and that, for a helical tube, the RTD curve is qualitatively similar, but narrower, than for a straight pipe. A few years later, Nauman [6] carried out a more detailed theoretical investigation of RTD in curved pipes, taking into account the incidence of molecular diffusion on the dispersion process; he showed that RTD curves exhibit a slowly converging tail, such as that computed by Ruthven [5]. Janssen [7] numerically studied longitudinal dispersion in laminar flow in helically coiled tubes in such conditions that molecular diffusion plays a dominating role. For Dean numbers, Dn, smaller than 16, the ratio between the dispersion coefficient in coils and in straight pipes is given as a function of the dimensionless group $\mathrm{Dn}^2 Sc$ for coil-pipe diameter ratios greater than 20. Using Monte-Carlo statistical simulation and numerical methods to solve the dispersion equation, Johnson and Kamm [8] evaluated Taylor dispersion in a curved duct for low Dean numbers ($\mathrm{Dn} \leq 17$) and curvature ratios less than 0.02 using Dean velocity profiles [2,3]. Janssen [7] and Johnson and Kamm [8] confirmed that $\mathrm{Dn}^2 Sc$ is in fact the appropriate parameter to discriminate between the different dispersion processes. For $\mathrm{Dn}^2 Sc$ less than 100, molecular diffusion drives the transport in the cross-sectional plane and D_{eff} remains the same as that obtained in straight pipes. When $\mathrm{Dn}^2\mathrm{Sc}$ increases, secondary flow effects dominate, inducing a decrease in D_{eff}.

Trivedi and Vasudeva [9] reported an experimental study on residence time distribution in the low-Reynolds number and low-

Dean number region (Dn ≤ 11) in helical coils having curvature ratios, R_c/D, ranging from 10.5 to 278. In these configurations, they obtained an essentially unique RTD curve which is narrower than that for straight ducts, confirming the theoretical results of Ruthven [5]. Trivedi and Vasudeva [10] complemented their previous experimental study by investigating the incidence of molecular diffusion for Schmidt numbers varying from 1500 to 8700, using the same coils as previously [9]. Depending on curvature ratio and Reynolds number, a 1.5- to 500-fold reduction in axial dispersion was observed compared with that in a straight tube; this reduction was enhanced by an increase in Schmidt number. Looking closely at the experimental data of Trivedi and Vasudeva [9], Saxena and Nigam [11] showed that a unique RTD was not really obtained, but rather a gradual narrowing of RTD curves with an increase in Dean number. Saxena and Nigam [11] argued that, starting with coils having large curvature ratios and for low Reynolds numbers, the RTD should shift from that for straight ducts to that for helical coils. To validate this assumption, they conducted a set of experiments using three coils with curvature ratios equal to 5.25, 113.15 and 332.8 and Dean numbers varying from 0.01 to 6.

In fact, two competing mechanisms of dispersion are present in helically coiled systems: (i) a dislocation, to the outer wall, of the maximum of the velocity profile (asymmetric profile) due to the curvature effects which increases the spread of residence time distribution; (ii) the secondary flow (Dean-roll cells) generates a transverse mixing that decreases axial dispersion. The relative balance between these two competing actions depends on the Reynolds number, since the effective dispersion first increases and then decreases with increasing *Re*. Nunge et al. [12] treated dispersion analytically using the velocity distribution of Topakoglu [13] in curved pipes. They showed that, for small Reynolds numbers, the effective dispersion may be substantially increased by curvature effects, though it remains of the same order of magnitude as that in the straight pipe. They also observed, for laminar flow in helical systems that the effective axial dispersion decreases with an increase in *Re* due to the secondary flow. However, a transition occurs for Reynolds numbers greater than 3000, for which the strength of the secondary flow becomes less important than axial velocity effects, especially for helical systems with small curvature, thus inducing an increase of the effective dispersion [14]. For still higher Reynolds numbers, the turbulent regime prevails and axial dispersion is reduced by turbulent mixing. Castelain et al. [15] compared axial dispersion in a helical system with that obtained in a straight pipe for Reynolds numbers greater than 2000 (turbulent flow). They showed that the effective dispersion in a helically coiled system in the laminar flow regime ($Re < 8000$) is of the same order of magnitude as that observed in a straight tube in turbulent flow regime. All experimental studies, notably those of Castelain et al. [15] in helical configuration, emphasize a narrowing of the residence time distribution compared with that in a straight tube. This conclusion was also confirmed by the numerical simulation of Castelain et al. [16]. Narusawa and Myamae [17] numerically investigated the relation between the flow parameters (tube length, hydraulic diameter, velocity flow) and the axial dispersion in a helix. They concluded that axial dispersion increases with the reactor length and with the residence time. This dispersion is reduced when the flow rate increases. However, since the trajectories in the secondary flow generated by Dean cells constitute an integrable system (in term of dynamical systems), a fluid particle always remains on a unique streamline and can change its trajectory only by means of molecular diffusion (a phenomenon called “regular mixing” hereafter).

Because of the integrability of the trajectories, two different laminar mixing regimes can exist: (i) regular mixing, for which the pathlines are integrable over the whole geometry. The flow in a helically coiled tube, in which a pair of secondary flow vortices with closed streamlines is formed under curvature effects, is of this kind; (ii) chaotic mixing, also called “irregular mixing”, in which pathlines are non-integrable and induce chaotic trajectories of fluid particles.

The flow regime associated with the latter case, frequently called chaotic advection, presents mixing properties comparable to those inherent to turbulent flow. The use of chaotic advection by introducing a geometrical perturbation between bends allows to a particle to follow a chaotic trajectory and consequently to move in the whole transversal section. Chaotic advection can appear for small Reynolds numbers and assists molecular diffusion in transverse mixing, thus decreasing the axial dispersion below its value for integrable system. These properties present a significant advantage for the mixing of very viscous or fragile fluids for which turbulence generation can cause damages and increase pumping costs due to pressure drops. The idea of generating a spatial (Lagrangian) chaotic behavior from a deterministic flow by simple geometrical perturbations has attracted much attention in recent years [18–20], mainly because of its potential application in mixing devices [21–23]. The geometrical perturbation induces complex three-dimensional chaotic trajectories in which particles can visit a large number of positions in physical space. To generate chaotic flow paths, the technique involved hereafter exploits the secondary flow patterns, usually known as Dean cells [20]. By shifting the plane of curvature of each successive bends, one can induce a class of trajectories in one bend, then deform it to another type in the next bend, and so on. Very complex flow paths can be produced this way, and a fluid particle undergoing such flows follows a chaotic path. The nature of the flow regime depends on the following conditions: (i) the angular extension of the bend; (ii) the angle between the planes of curvature of two successive bends; (iii) the global rotation protocol and finally; (iv) the Dean number. For instance, when the geometrical perturbation remains small, some streamlines are confined in streamtubes where the flow remains regular, whereas other trajectories become chaotic; this is the mixed regime. If the whole trajectories become non-integrable, the flow is called fully chaotic.

In previous works, Castelain et al. [15,16] compared RTD in helically coiled and chaotic twisted pipes for Reynolds numbers ranging from 30 to 13,000, for different bend numbers, using Newtonian fluids. Water was used as the working liquid for Reynolds numbers greater than 800 and two saccharose solutions for Reynolds numbers ranging from 30 to 1700. In order to investigate the dispersion phenomenon in the two experimental arrangements, Castelain et al. [15,16] used the axial dispersion plug flow model. For Reynolds numbers larger than 2500, axial dispersion in the chaotic system is more than 20% smaller than in a helically coiled tube having the same number of bends. The decrease in axial dispersion is due to the generation of chaotic trajectories, which also contributes to an increase in transverse dispersion. Chaotic advection helps molecular diffusion in the transverse mixing and reduces axial dispersion. This reduction is due to chaotic trajectories which allow the particles to sample more quickly the axial velocity profile. For smaller Reynolds numbers, the fitting between the plug flow with axial dispersion model and the experimental RTD curves was not satisfactory, mainly due to the long tails appearing on the experimental RTDs. Thus, for Reynolds numbers less than 2500, the experimental RTD of a Newtonian fluid was modeled using a plug flow with axial dispersion part exchanging mass with a stagnant region and the axial dispersion was less important in chaotic configuration too. Saxena et al. [24] measured the residence time in a laminar flow to characterize the performances of various mixers configurations with different bend shifts. For Reynolds numbers varying from 30 to 150, they showed that the residence time distribution is very sensitive to the rotation protocol, the best results being obtained for a 90° angle shift between two successive bends.

Most of the studies dealing with mixing characterization in helical configurations are dedicated to Newtonian fluid flows. The few works carried out using non-Newtonian fluids are only concerned with the helical configuration. Singh and Nigam [25] have measured the RTD in two helical mixers of same length but with different curvature aspect ratios. The used pseudoplastic fluids were aqueous solutions with carboxymethyl cellulose (CMC) concentrations of 1% and 2% in weight. RTD was obtained by means of a colored tracer (Congo red dye) detected by colorimetry for generalized Reynolds numbers varying between 0.01 and 2.5. For non-Newtonian fluids, the generalized Reynolds number is defined in such a way that the relation between the friction factor and the Reynolds number for laminar isothermal flow of Newtonian fluids is the same as for non-Newtonian fluids [26]. The experimental data of Singh and Nigam [25] have been correctly modeled using the plug flow with axial dispersion model for pseudoplastic fluids in helical systems. Saxena et al. [24] numerically observed a narrowing of the residence time distribution in a helical system with the decrease of the flow behavior index of a pseudoplastic fluid ($0.2 \leq n \leq 2$). They experimentally verified their results using five different CMC solutions ($0.6 \leq n \leq 1$) for Reynolds numbers extending from 0.1 to 140. The same results were also numerically obtained by Ranade and Ulbrecht [27] for n ranging from 0.2 to 1.5.

The present work describes an experimental study of residence time distributions (RTD) of a pseudoplastic fluid for different configurations of a helically coiled system and a chaotic one based on alternated curved ducts for generalized Reynolds numbers varying between 30 and 260. In order to investigate dispersion in the two experimental arrangements, we used the axial dispersion model exchanging mass with a stagnant zone. The experimental apparatus and methods are described in the next section. The third section covers the modeling of the experimental RTD, while the fourth one deals with the analysis, the discussion of the experimental data and the comparison with the results obtained for Newtonian fluids.

2. Experimental apparatus and methods

2.1. Flow loop

The experimental flow loop, previously described in Castelain et al. [15,16] consists of an overhead reservoir from which the working fluid is circulated by means of a helical shaft pump. The flow rate is measured by an electromagnetic flowmeter, with an accuracy of ±1.5 % over the whole flow range. Before entering the chaotic or the helically coiled system, the liquid flows through a straight pipe 3 m long, more than 65 times the inner diameter of the curved tubes, ensuring a fully developed axial flow at the inlet of the test section for the range of Reynolds numbers under investigation ($30 \leq Re \leq 270$).

The helical and chaotic mixers are both made of identical bends. Each bend consists of a 90° curved stainless-steel tube of circular cross section, the inner and outer radii of which are 23 and 25 mm, respectively. The mean radius of curvature of the bends is 126.5 mm, which yields a mean curvature ratio of 0.18. The bends can be assembled so as either to form a helically coiled pipe or to generate chaotic pathlines. The complete helical system consists of 33 bends, connected by 16 straight sections of 55 mm length (Fig. 1a). The chaotic twisted pipe device is

(a)

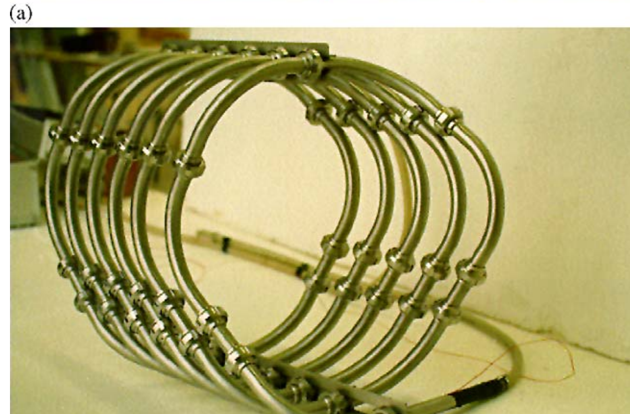

(b)

Fig. 1. The two systems under study : (a) helically coiled tube; (b) chaotic configuration.

Table 1
Geometrical parameters of the studied configurations

Lengths of the studied configurations			
Number of bends	Curved length (m)	Straight length (m)	Total length (m)
Hellically coiled system			
3	0.596	0.295	0.891
9	1.788	0.935	2.723
15	2.981	1.585	4.566
21	4.173	2.230	6.403
27	5.365	2.875	8.240
33	6.557	3.521	10.078
Chaotic system			
3	0.596	0.320	0.916
6	1.192	0.640	1.832
9	1.788	0.960	2.748
15	2.981	1.600	4.581
21	4.173	2.240	6.413
27	5.365	2.880	8.245
33	6.557	3.520	10.078

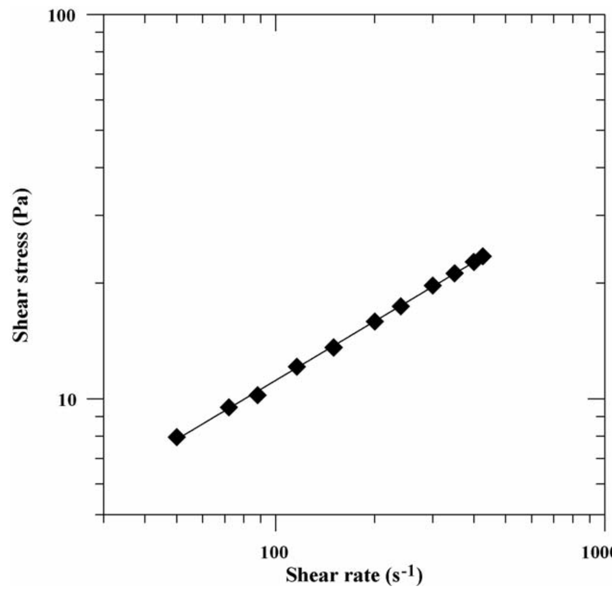

Fig. 2. CMC rheological behavior.

also made of 33 bends and 11 straight sections of 80 mm length (Fig. 1b). The latter geometry is obtained by shifting the plane of curvature of each bend by a ±90° angle with respect to the neighboring ones. Different configurations, made up with 3–33 bends, were tested (Table 1).

2.2. Working fluid

In our previous works [15,16], water and saccharose Newtonian solutions were used as working fluids for Reynolds numbers ranging from 30 to 13,000 (Table 2). In the present study, a purely viscous non-Newtonian liquid is used, carboxymethyl cellulose (CMC) 7H4C at a mass concentration of 1%. The CMC solution is made in small batches of 20 l. The rheology of each batch is measured with a Weissenberg rheometer at imposed shear rate using a cone and plate measurement system. All batches are mixed in a reservoir. The global fluid rheology is regularly controlled and the CMC solution is changed when its rheology begins to vary. At a temperature equal to 20 °C, the rheologic behavior of all the solutions follows, on average, an Ostwald-de-Waele law, whose consistency, k, is equal to 0.96 Pa s^n, the flow behavior index, n, being equal to 0.52 (Fig. 2). During the residence time distribution (RTD) experiments, the working liquid is not recycled so as to avoid any modification of its physical properties, but is instead stored in a second reservoir.

2.3. Determination of the residence time distribution

The RTD of a passive tracer was obtained using a conductimetric method with two measurement points [15,16]. The concentration of an injected tracer was sampled, as a function of time, at both the inlet and the outlet of the geometry under study. To ensure a uniform tracer concentration at the entrance of the twisted pipe, the tracer injection was followed by a seven-element Sulzer SMX static mixer, which extends the time distribution of the tracer at the inlet in order to allow a correct sampling of the entrance concentration signal.

The passive tracer was detected using two specially designed conductimetric cells made up of two semicylindrical nickel plates insulated from each other and having the same diameter as the twisted pipe systems. Each sensor is connected to a variable-frequency conductimeter (TACUSSEL CD 810). The frequency of the applied alternating current between the two electrodes of the conductimetric cells was fixed to 1 kHz in order to ensure a linear relationship between the conductivity and the concentration of the tracer. The concentration curves at the inlet, $C_1(t)$,

Table 2
Hydrodynamical parameters of the studied configurations

Experimental domain			
System	Number of bends	Viscosity of the liquid (Pa s)	*Re* range
Castelain et al. [15]			
Helically coiled	3, 9, 15, 21, 27, 33	10^{-3} (water)	800–13000
Chaotic	3, 9, 15, 21, 27, 33	10^{-3} (water)	800–13000
Castelain et al. [16]			
Chaotic	3, 6, 9, 33	0.102–0.128 (saccharose)	30–200
Chaotic	3, 6, 33	0.012 (saccharose)	400–1700

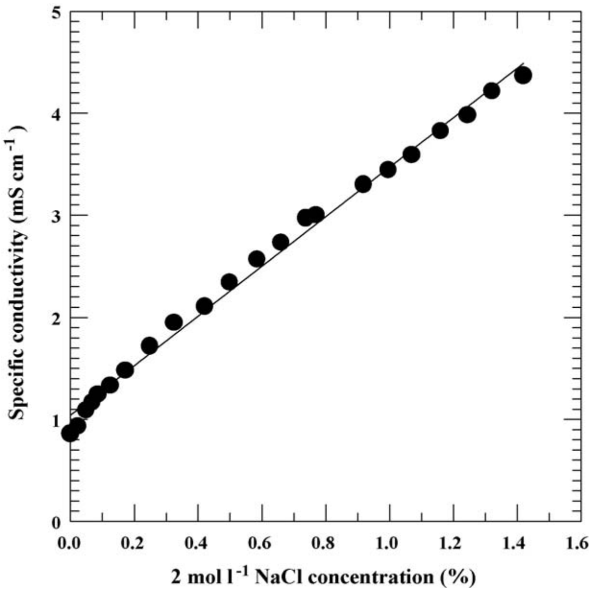

Fig. 3. Specific tracer conductivity vs. 2 mol l^{-1} NaCl concentration.

and at the outlet, $C_2(t)$, of the system are sampled at a frequency varying between 7 and 60 Hz (depending on the flow rate) by means of a data-acquisition device (AOIP SA 32) connected to a personal computer for data processing.

After Li and Choplin [28], the lack of experimental data dealing with residence time distribution of non-Newtonian fluids in various industrially-used devices is mainly due to the difficulty of finding a tracer which does not interact with the working fluid in order to maintain the initial properties of the non-Newtonian liquid. The used tracer must not alter the fluid and must have a sufficient specific conductivity to be detected, which furthermore has to evolve linearly with the concentration.

The attempts with a NaOH solution, used as tracer for Newtonian fluids, showed an important and immediate degradation of the long and fragile CMC molecules. Different tracers were tested. A 2 mol l^{-1} NaCl solution was found to be suitable, avoiding any modification of the characteristics of the CMC solution. The specific conductivity was measured using the same conductimetric cell, but closed at the entrance and at the exit. This specific conductivity evolution of the tracer solution versus the NaCl concentration, presented in Fig. 3, is linear. In order to reduce flow perturbation, the injected tracer viscosity has to be adjusted to that of the CMC solution. The apparent viscosity of a pseudoplastic liquid, such as the CMC solution used hereafter, varied as a function of the applied shear rate. Thus, the viscosity of the tracer solution was adjusted to the mean value of the CMC one ($\mu = 0.1$ Pa s) using a viscous Newtonian liquid, EMKAROX HV 45, which is totally soluble in water. Rheological measurements of the CMC solution after the injection of the NaCl tracer have been made and showed that the tracer solution injection does not alter the properties of the initial CMC solution. The use of a 50% w/w concentration of EMKAROX HV45 and NaCl 2 mol l^{-1} aqueous solution allowed to maintain the desired apparent viscosity of the working fluid. After each determination of the RTD, the rheological properties of the fluid were checked, the CMC solution being changed if any modification of its rheology was observed. The injected volume of NaCl was about 2 cm^3.

3. Modeling of the residence time distribution

In a previous work, Castelain et al. [15] used the axial dispersed plug flow model to characterize RTD curves of a Newtonian liquid flowing through the same devices used here for high Reynolds numbers ($2500 \leq Re \leq 13000$). For this Reynolds numbers range, the flow in the chaotic twisted pipe arrangement can be considered as fully chaotic in the whole section of the apparatus [15,19]. In this case, the dispersed plug flow model has been found suitable for a correct prediction of the RTD of the liquid, both in the chaotic and in the helically coiled systems [15], confirming previous experimental works dedicated to the latter configuration [9,10,21].

As previously observed by Castelain et al. [15,16], for Reynolds numbers less than about 2500, the agreement between the plug flow with axial dispersion model and the experimental RTD in the chaotic curved-pipe arrangement is not as satisfactory as for Reynolds numbers greater than 2500, when using a Newtonian fluid. This is mainly due to the tails of the experimental RTD, which cannot be correctly predicted using the dispersed plug flow model. These tails were also observed by Jones and Young [29] in a theoretical investigation of dispersion of a passive scalar in steady viscous flow through a twisted pipe subjected to chaotic advection. The flow can thus be considered as a mixed regime in which islands of integrable trajectories coexist within irregular regions [19,29]. The trajectories of fluid particles do not instantaneously become fully chaotic as the fluid enters the twisted pipe system. At the inlet, small regions where the flow becomes less and less regular appear. They spread along the flow path to finally sample the whole cross-section. The transition between these asymptotic flow regimes is characterized by the coexistence of chaotic zones with regular parts; this competition induces tails on the RTD curves. Thus, for Reynolds numbers less than about 2500, the experimental RTD of a Newtonian liquid was modeled using a plug flow with axial dispersion part that exchanges mass with stagnant region [16]. This model is expressed by the two following differential equations [30]:

$$D_{\mathrm{ax}}\frac{\partial^2 C}{\partial z^2} - \bar{W}\frac{\partial C}{\partial z} = f\frac{\partial C}{\partial t} + (1-f)\frac{\partial C^*}{\partial t} \quad (1)$$

$$(1-f)\frac{\partial C^*}{\partial t} = K(C - C^*) \quad (2)$$

C is the tracer concentration in the flowing part of the device in which $\bar{W}$ the mean velocity and D_{ax} the axial dispersion coefficient. C^* is the tracer concentration in the stagnant zone, f the fraction of volume subjected to plug flow with axial dispersion, and K is the mass transfer coefficient between the flowing volume and the stagnant region.

The characteristic parameters of this flow model are determined using curve-fitting in the time domain [31,32]. This appears to be the most accurate way to identify the different parameters involved in a given flow model from measurement of tracer input and response signals [33]. This method is based on the comparison of the experimental concentration outlet curve and that calculated, in the time domain, using the inlet curve concentration signal and the transfer function of the flow model. The inlet, $C_1(t)$, and outlet, $C_2(t)$, concentration curves are first normalized to ensure exact satisfaction of the tracer balance, and then expressed in terms of Fourier series. The resolution of Eqs. (1) and (2), using the Laplace transform, allows the determination of the transfer function, $F(s) = C_{2\text{calc}}(s)/C'_1(s)$, between Laplace transforms of the normalized calculated outlet signal and the experimental inlet curve, given by:

$$F(s) = \frac{2\beta^{1/2}\exp\left\{\frac{1}{2}[Pe_\text{L} - \beta^{1/2}]\right\}}{(Pe_\text{L} + \beta^{1/2}) - (Pe_\text{L} - \beta^{1/2})\exp\{-\beta^{1/2}\}} \tag{3}$$

with $\beta = Pe_\text{L}^4 + 4s\gamma Pe_\text{L}\bar{t}_\text{s}$ where $\bar{t}_\text{s}$ is the mean residence time of the fluid in the system; $\gamma = f + (G(1-f)/\bar{t}_\text{s}(1-f)s + G)$; $G = KL/\bar{W}$. $Pe_\text{L} = \bar{W}L/D_\text{ax}$ is the Péclet number in the flowing part of the device of total length L.

This model involves four parameters, $\bar{t}_\text{s}$, G, f and Pe_L, the optimization of which is very difficult without a good initial estimate. The complete procedure is described in Castelain et al. [16]. The predicted temporal normalized response concentration curve, $C'_{2\text{calc}}(t)$, can thus be calculated using the definition of the transfer function in the Fourier domain and the normalized inlet signal, $C'_1(t)$:

$$F(\mathrm{i}\omega) = \frac{\int_0^{2T} C'_{2\text{calc}}(t)\exp(-\mathrm{i}\omega t)\,\mathrm{d}t}{\int_0^{2T} C'_1(t)\exp(-\mathrm{i}\omega t)\,\mathrm{d}t} \tag{4}$$

ω being the pulsation of the Fourier series and $2T$ the time in which the tail of the response signal, $C'_2(t)$, vanishes.

The experimental, $C'_2(t)$, and predicted, $C'_{2\text{calc}}(t)$, response curves are compared by evaluating the root mean square error, RMS, between these two signals [32]:

$$\text{RMS} = \left[\frac{\int_0^{2T}[C'_2(t) - C'_{2\text{calc}}(t)]^2\,\mathrm{d}t}{\int_0^{2T}[C'_2(t)]^2\,\mathrm{d}t}\right] \tag{5}$$

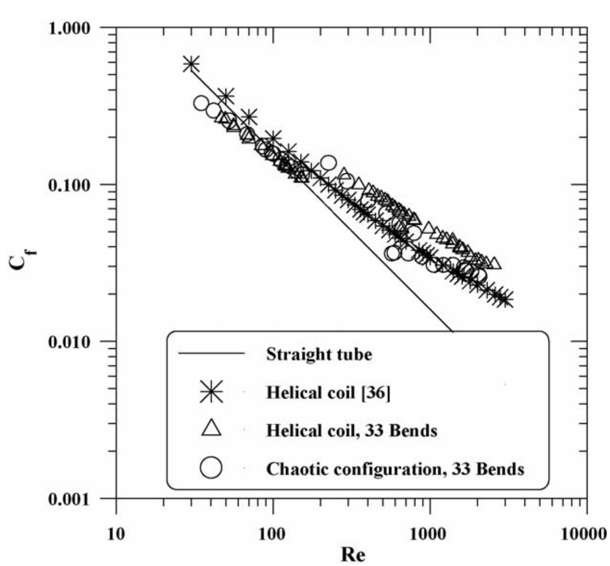

Fig. 4. Friction factor vs. Reynolds number.

RMS, which is a function of the four parameters of the model, is minimized using the Rosenbrook optimization algorithm [34].

4. Results and discussion

For non-Newtonian fluids, the generalized Reynolds number is established so that the relation between the friction factor and the Reynolds number for non-Newtonian fluids remains the same as that for laminar isothermal flow of Newtonian fluids [26]. The relation between the friction factor and the Reynolds number for laminar isothermal flow of Newtonian fluids in ducts is given by:

$$\frac{C_\text{f}}{2} = \frac{2\tau_\text{w}}{\rho\bar{W}^2} = \frac{2}{\rho\bar{W}^2}\frac{D\Delta P}{4L} = \frac{\xi}{Re} \tag{6}$$

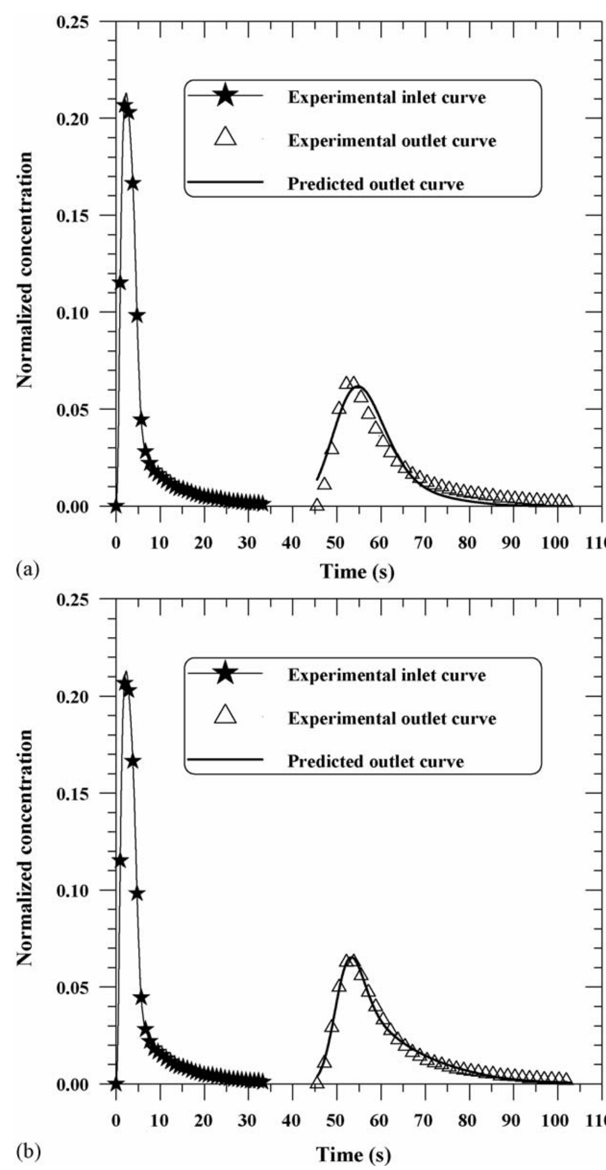

Fig. 5. An example of curve-fitting in time domain using the two models (33-bend chaotic system): (a) plug flow model with axial dispersion; (b) dispersed plug flow model exchanging mass with a stagnant zone.

where C_f is the friction factor, ΔP the pressure drop, L the length of the channel, $\bar{W}$ the mean flow velocity and ξ is a dimensionless geometrical parameter whose value for different ducts configurations is given by Shah and London [35]. The Dean number for non-Newtonian fluids is defined as:

$$\mathrm{Dn_g} = Re_g\sqrt{\frac{D}{R_c}} \qquad (7)$$

In order to determine the ξ factor of the two configurations, the pressure drops, for a Newtonian fluid, have been measured using a differential Schlumberger pressure sensor. The principle of measurement is as follows: the upstream and downstream pressures are transmitted to the sensor by a secondary fluid (water). These two pressures are transmitted to two separating membranes. The resulting pressure, hence the differential pressure, is transmitted to a third membrane, called measurement membrane, which supports the detector. The latter measures a magnetic core micro-displacement placed in the magnetic field. The calibration consists in comparing, for example, the signal of the sensor with that obtained using a differential water column manometer. The friction factor, C_f, is given in Fig. 4 as a function of the Reynolds number for the two studied configurations having 33 bends and for a straight tube and a helical coil investigated by Singh and Mishra [36]. For Reynolds numbers lower than 110, the friction factor for the two configurations studied here is of the same order of magnitude as that obtained in a straight tube. This is in agreement with other correlations existing for the friction factor in helical coils. One can thus consider that the factor ξ is the same as for a straight tube and thus equal to 1. In this case, the generalized Reynolds number is given by [26]:

$$Re_g = 8^{1-n}\left[\frac{4n}{3n+1}\right]^n \frac{\rho \bar{W}^{2-n} D^n}{k} \qquad (8)$$

Measurements have been realized for various configurations of a chaotic and helical system for a range of generalized Reynolds numbers between 30 and 260. As in the study of the residence time distribution for Newtonian fluids for small Reynolds numbers, the agreement between the plug flow with axial dispersion model and the experimental residence time distributions is not satisfactory. To take into account the tails of the experimental RTD, we chose to use a plug flow model with axial dispersion part that exchanges mass with a stagnant region. An example of curve-fitting is given in Fig. 5 for a 33-bend configuration system. The RMS is equal to 21.8% if the plug flow with

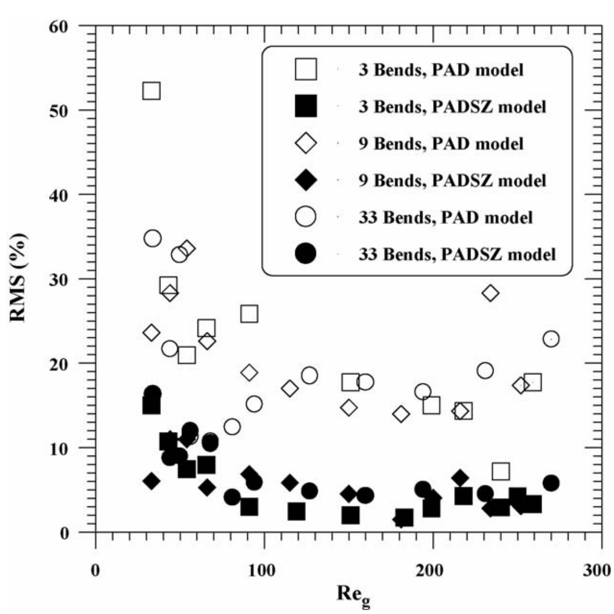

Fig. 6. Accuracy of the two flow models for the prediction of RTDs in chaotic configuration. PAD: plug flow with axial dispersion model; PADSZ: plug flow with axial dispersion model exchanging mass with a stagnant zone.

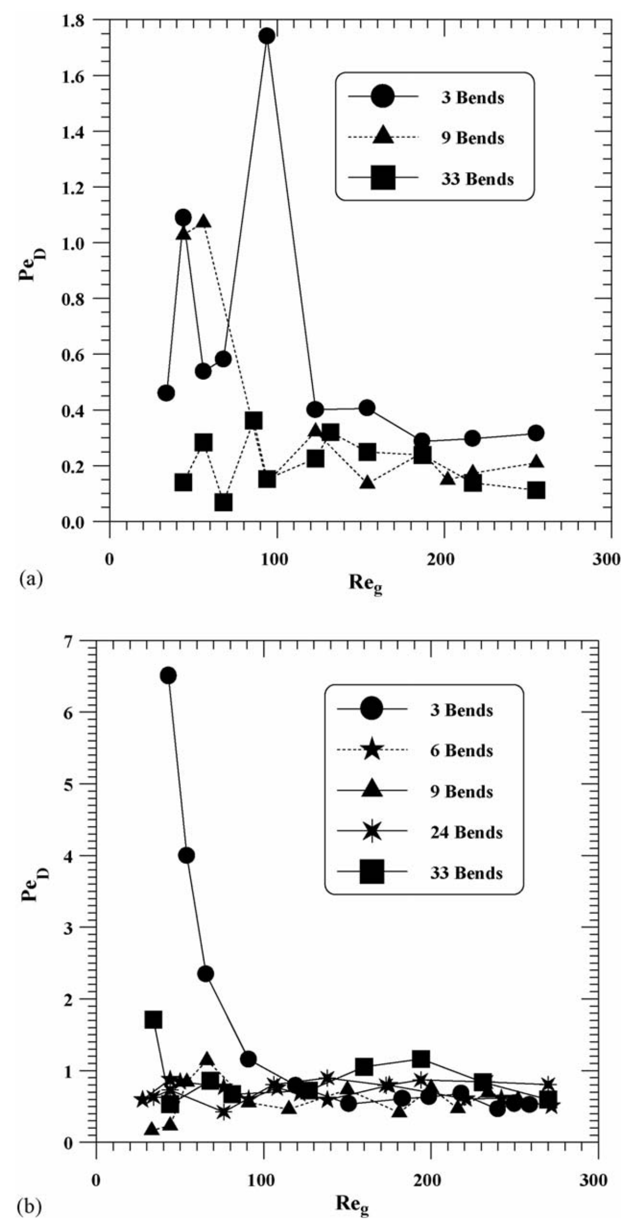

Fig. 7. Péclet number based on the diameter vs. Reynolds number for different configurations: (a) helically coiled configuration; (b) chaotic configuration.

axial dispersion model is used (Fig. 5a), whereas it is reduced to 5% with the dispersed plug flow model exchanging mass with a stagnant zone (Fig. 5b). The use of the plug flow model with axial dispersion part that exchanges mass with a stagnant region allows to obtain a root mean square error between the experimental and modeled outlet signals lower than 10% (Fig. 6).

The variation of the Péclet number based on the pipe diameter, $Pe_{\mathrm{D}} = (\bar{W}D/D_{\mathrm{ax}})$, versus the Reynolds number in chaotic or helical configurations is given in Fig. 7. In helical configuration, the Péclet number decreases with the number of bends constituting the system, but seems to be only slightly dependent on the Reynolds number, especially for Re_{g} greater than 100. The increase of the number of bends seems to enhance axial dispersion.

In chaotic configuration, the Péclet number is globally stable around a value of 0.8. Thus this parameter is not very sensitive to the number of bends and to the Reynolds number, except for the three bends configuration, for which the small length of the system coupled with the chaotic mixing reduce axial dispersion.

The Péclet number based on the diameter is more important in the chaotic geometry than in the helical one, particularly for Reynolds numbers smaller than 100. As a high Péclet number indicates a small axial dispersion, the dispersion is smaller in chaotic configuration. In chaotic system, the reduction of the axial dispersion is more pronounced because of the set-up of chaotic trajectories in the flow. This phenomenon accounts for an increase in transverse dispersion. The results are in agreement with those obtained for Newtonian fluids by Castelain et al. [16].

Fig. 8 represents the evolution of the flow fraction in the two systems versus Reynolds number. The flow fraction increases with the number of bends in both configurations. The increase of the system length induces better fluid mixing. In the two systems, the flow fraction increases with the Reynolds number up to a Reynolds number around 100. Even if the secondary flow is present for smaller Reynolds numbers, it is weaker. Consequently, the particles located near the wall find it difficult to move near the center of the section. The strength of the secondary flow increases with the Reynolds number and helps particles displacement. The comparison between the flow fraction in the two configurations shows the reduction of the volume of the dead zones, hence the mixing increase, for the chaotic configuration. This enhancement is more and more important with the increase of the system length. In chaotic configuration, the maximum value is reached for a Reynolds number lower than in helicoïdal configuration.

Fig. 9 presents the comparison between the variations of the Péclet number based on the pipe diameter for a Newtonian fluid obtained by Castelain et al. [15] and that measured for the pseudoplastic fluid. The values of the Péclet number are greater for the non-Newtonian fluid, because of the local change in appar-

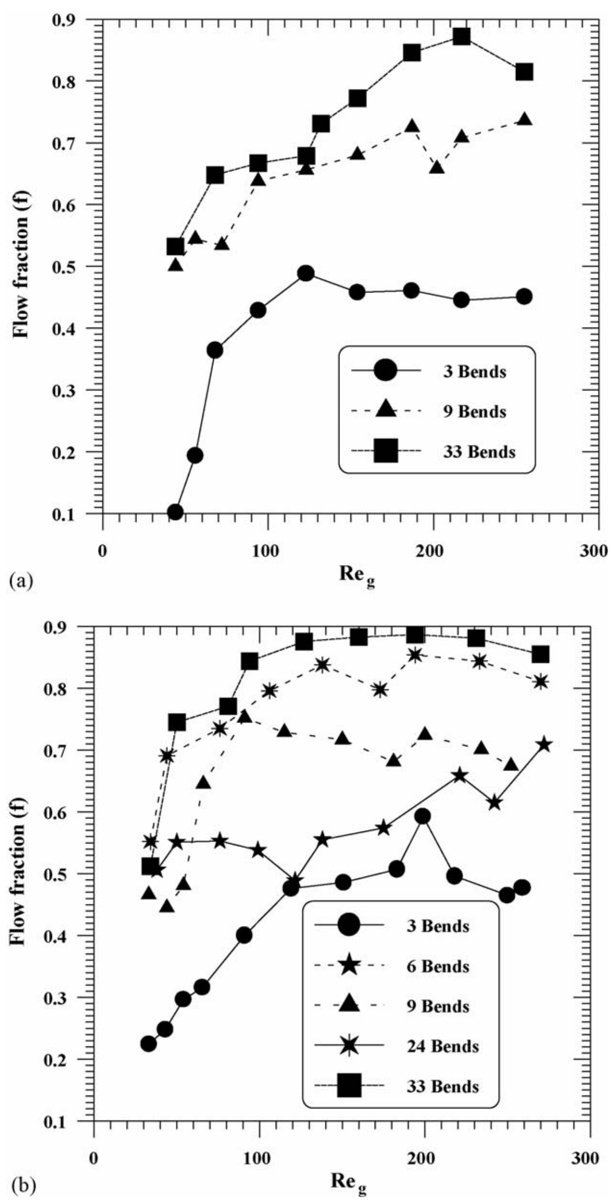

Fig. 8. Variation of the flow fraction vs. Reynolds number: (a) helically coiled configuration; (b) chaotic configuration.

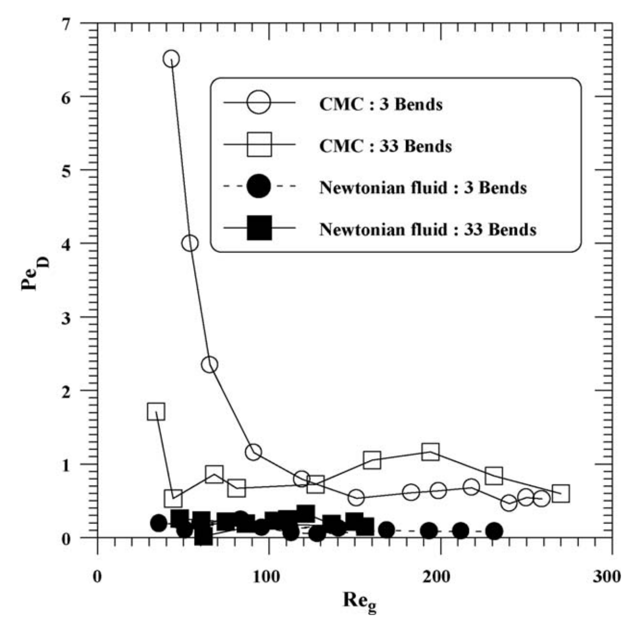

Fig. 9. Comparison of the Péclet number in chaotic configuration for Newtonian and pseudoplastic fluids.

ent viscosity which affects the secondary flow. For pseudoplastic fluids, the apparent viscosity is reduced near the wall and higher at the center of the cross section. Agrawal et al. [37] showed that pseudoplasticity decreases the intensity of the secondary flow. In the plane of curvature, the axial velocity profile exhibits a single peak shifted toward the concave wall due to centrifugal force. When the flow behavior index decreases, the shift of the axial velocity profile toward the concave wall is more pronounced, thereby inducing a globally more flatten velocity profile, hence a smaller axial dispersion, than for the Newtonian fluid. The maximum axial velocity decreases as the flow behavior index is reduced, so that the pseudoplastic fluids cause the attenuation of the secondary flow in the center of the tube and the increase of the secondary flow near the wall. The works of Singh and Nigam [25] and Ranade and Ulbrecht [27] also emphasized the acceleration of the secondary flow near the wall which reduces axial dispersion.

5. Conclusion

The experimental evaluation of the residence time distribution in a helical system and in a spatially chaotic system associated with the use of a plug flow model with axial dispersion part exchanging mass with a stagnant region, has allowed the determination of an effective axial dispersion coefficient in the two configurations in the case of a pseudoplastic fluid and for Reynolds numbers lower than 300. A tracer and a detection method have been used successfully. The obtained results confirmed that simple plug flow with axial dispersion model is not adapted to the small Reynolds numbers, even for a pseudoplastic fluid. In the case of the helical system, the results are in good agreement with the literature. In the chaotic system, axial dispersion is reduced compared with that in the helical configuration. The decrease in axial dispersion is due to the generation of chaotic trajectories in the flow. This phenomenon also contributes to the increase in transverse dispersion because, before leaving the system, fluid elements visit a large sample of transverse positions with different velocity values. This is not the case in the helically coiled tube system, in which fluid elements are trapped in regular streamlines. The results show that, for the same generalized Reynolds number, axial dispersion is reduced in the case of the pseudoplastic fluid. Even if the secondary flow is reduced in the center of the tube, the increase of the secondary flow near the walls, due to the decrease of the apparent viscosity in this region, reduces the residence time, particularly for particles located near the walls and for small Reynolds numbers.

These results are encouraging for the use of this system as continuous mixer for complex fluids in laminar regime, particularly for small Reynolds numbers, where the friction factor is of the same order of magnitude as that measured in a straight tube.

References

[1] G.I. Taylor, Dispersion of soluble matter in solvent flowing slowly through a tube, Proc. Roy. Soc. Lond. A219 (1953) 186–203.
[2] W.R. Dean, Note on the motion of fluid in a curved pipe, Philos. Mag. 4 (1927) 208–227.
[3] W.R. Dean, The stramline motion of fluid in curved pipe, Philos. Mag. 5 (1928) 673–695.
[4] M.E. Erdogan, P.G. Chatwin, The effects of curvature and buoyancy on the laminar dispersion of solute in a horizontal tube, J. Fluid Mech. 29 (1967) 465–484.
[5] D.M. Ruthven, The residence time distribution for ideal laminar flow in helical coil, Chem. Eng. Sci. 26 (1971) 1113–1121.
[6] E.B. Nauman, The residence time distribution for laminar flow in helically coiled tubes, Chem. Eng. Sci. 32 (1977) 287–293.
[7] L.A.M. Janssen, Axial dispersion in laminar flow through coiled tubes, Chem. Eng. Sci. 31 (1976) 215–218.
[8] M. Johnson, R.D. Kamm, Numerical studies of steady flow dispersion at low Dean number in a gently curved tube, J. Fluid Mech. 172 (1986) 329–345.
[9] R.N. Trivedi, K. Vasudeva, RTD for diffusion-free laminar flow in helical coils, Chem. Eng. Sci. 29 (1974) 2291–2295.
[10] R.N. Trivedi, K. Vasudeva, Axial dispersion in laminar flow in helical coils, Chem. Eng. Sci. 30 (1975) 317–325.
[11] A.K. Saxena, K.P.D. Nigam, On RTD for laminar flow in helical coils, Chem. Eng. Sci. 34 (1979) 425–426.
[12] R.J. Nunge, T.S. Lin, W.N. Gill, Laminar dispersion in curved tubes and channels, J. Fluid Mech. 51 (1972) 368–383.
[13] H.C. Topakoglu, Steady laminar flows of an incompressible viscous fluid in curved pipes, J. Math. Mech. 16 (1967) 1321–1338.
[14] J.A. Koutsky, R.J. Adler, Minimization of axial dispersion by use of the secondary flow in helical tubes, Can. J. Chem. Eng. (1964) 239–246.
[15] C. Castelain, A. Mokrani, P. Legentilhomme, H. Peerhossaini, Residence time distribution in twisted pipe flows: helically coiled and chaotic systems, Exp. Fluids 22 (1997) 359–368.
[16] C. Castelain, D. Berger, P. Legentilhomme, A. Mokrani, H. Peerhossaini, Experimental and numerical characterisation of mixing in a spatially chaotic flow by means of residence time distribution measurements, Int. J. Heat Mass Transfer 43 (2000) 3687–3700.
[17] Y. Narusawa, Y. Myamae, Evidence of axial dispersion accompanied by axial dispersion with zone circulating flow-injection analysis data, Anal. Chim. Acta 309 (1995) 227–239.
[18] H. Aref, Stirring by chaotic advection, J. Fluid Mech. 143 (1984) 1–21.
[19] S.W. Jones, O.M. Thomas, H. Aref, Chaotic advection by laminar flow in twisted pipe, J. Fluid Mech. 209 (1989) 335–357.
[20] Y. Le Guer, H. Peerhossaini, Order breaking in Dean-flow, Phys. Fluids A 3 (1991) 1029–1032.
[21] A.K. Saxena, K.P.D. Nigam, Axial dispersion in laminar flow of polymer solutions through coiled tubes, J. Appl. Polym. Sci. 26 (1981) 3475–3486.
[22] J.M. Ottino, The Kinematic of Mixing, Cambridge University Press, Cambridge, 1989.
[23] E. Villermaux, J.P. Hulin, Chaos Lagrangien et mélange de fluides visqueux, Eur. J. Phys. 11 (1990) 179–183.
[24] A.K. Saxena, K.M. Nigam, K.P.D. Nigam, RTD for diffusion-free laminar flow of non-Newtonian fluids through coiled tubes, Can. J. Chem. Eng. 61 (1983) 50–52.
[25] D. Singh, K.D.P. Nigam, Laminar dispersion of polymer solutions in helical coils, J. Appl. Polym. Sci. 26 (1981) 785–790.
[26] A.B. Metzner, J.C. Reed, Flow of non-Newtonian fluids: correlation of the laminar, transition and turbulent-flow regions, AIChE J. 1 (1955) 434–440.
[27] V.R. Ranade, J.J. Ulbrecht, Velocity profiles of Newtonian and non-Newtonian toroidal flows measured by a LDA technique, Chem. Eng. Commun. 20 (1982) 253–272.
[28] H.Z. Li, L. Choplin, Residence Time Distribution in Rheologically Complex Fluids. A survey, Dechema Monographs, vol. 127, VCH, Berlin, 1992, pp. 21–29.
[29] S.W. Jones, W.R. Young, Shear dispersion and anomalous diffusion by chaotic mixing, J. Fluid Mech. 280 (1994) 149–172.
[30] K.H. Coats, B.D. Smith, Dead end pore volume and dispersion in porous media, Soc. Pet. Eng. J., Trans. AIME 231 (1964) 73–84.

[31] W.C. Clements, A note on determination of the parameters of the longitudinal dispersion model from experimental data, Chem. Eng. Sci. 24 (1969) 957–963.
[32] N. Wakao, S. Kaguei, Heat and Mass Transfer in Packed Beds, Gordon and Breach Publishers, London, 1982.
[33] M.A. Fahim, L.T. Wakao, Parameter estimation from tracer response measurements, Chem. Eng. J. 25 (1982) 1–8.
[34] G.S.G. Beveridge, R.S. Schechter, Optimization: Theory and Practice, McGraw-Hill, New York, 1970.
[35] R.K. Shah, A.L. London, Laminar Flow Forced Convection in Ducts, Academic Press, New York, 1978.
[36] R.P. Singh, P. Mishra, Friction factor for Newtonian and non-Newtonian fluid flow in curved pipes, J. Chem. Eng. Jpn. 13 (1980) 275.
[37] S. Agrawal, G. Jayaraman, V.K. Srivastava, K.D.P. Nigam, Power law fluids in a circular curved tube. Part I. Laminar flow, Polym. Plast. Technol. Eng. 32 (6) (1993) 595–614.